The effect of a background shear current on large amplitude internal solitary waves

Wooyoung Choi[a)]
Department of Mathematical Sciences, Center for Applied Mathematics and Statistics, New Jersey Institute of Technology, Newark, New Jersey 07102-1982

(Received 18 October 2005; accepted 24 January 2006; published online 14 March 2006)

Large amplitude internal waves interacting with a linear shear current in a system of two layers of different densities are studied using a set of nonlinear evolution equations derived under the long wave approximation without the smallness assumption on the wave amplitude. For the case of uniform vorticity, solitary wave solutions are obtained under the Boussinesq assumption for a small density jump, and the explicit relationship between the wave speed and the wave amplitude is found. It is shown that a linear shear current modifies not only the wave speed, but also the wave profile drastically. For the case of negative vorticity, when compared with the irrotational case, a solitary wave of depression traveling in the positive x direction is found to be smaller, wider, and slower, while the opposite is true when traveling in the negative x direction. In particular, when the amplitude of the solitary wave propagating in the negative x direction is greater than the critical value, a stationary recirculating eddy appears at the wave crest. © *2006 American Institute of Physics*. [DOI: 10.1063/1.2180291]

I. INTRODUCTION

Large amplitude internal waves are no longer rare phenomena evidenced by an increasing number of field observations and the study of their physical properties has been an active research area in recent years; for example, see Lynch and Dahl,[1] Ostrovsky and Stepayants,[2] and Helfrich and Melville.[3] Classical weakly nonlinear theories including the well-known Korteweg–de Vries (KdV) equation have been found to fail in this strongly nonlinear regime, and it has been suggested that new theoretical approaches are necessary to better describe large amplitude internal waves.

These strongly nonlinear waves have often been studied numerically for both continuously stratified and multilayer fluids (Lamb;[4] Grue *et al.*[5]). Alternatively, with the long wave approximation but no assumption on the wave amplitude, the strongly nonlinear asymptotic models were proposed (Miyata;[6] Choi and Camassa;[7] Choi and Camassa[8]), and it was found that these simplified models are indeed valid for large amplitude waves. In particular, for traveling waves, the system of coupled nonlinear evolution equations can be reduced to a single ordinary differential equation, and its solitary wave solution shows excellent agreement with laboratory experiments and numerical solutions of the Euler equations (Camassa *et al.*[9]). The success of this asymptotic model even for large amplitude waves can be attributed to the fact that the internal solitary wave becomes wider as the wave amplitude increases and, therefore, the underlying long wave assumption is valid even for large amplitude waves.

Many of these previous studies have neglected the background shear current effect, which is important in real ocean environments but is not well understood. In this paper, the strongly nonlinear model is further generalized to include the shear current effect, and its solitary wave solutions and their wave characteristics are studied.

For continuously stratified flows, Maslowe and Redekopp[10] considered weakly nonlinear internal waves in shear flows and showed that the KdV and Benjamin-Ono equations can be derived for long waves in the shallow and deep configurations, respectively, both with and without critical layers. Stastna and Lamb[11] investigated numerically the effect of shear currents on fully nonlinear internal waves. For a linear shear current of negative constant vorticity, they found the internal solitary wave of elevation traveling in the positive x direction is taller and narrower, while the wave propagating in the opposite direction becomes shorter and wider. Their numerical solutions showed that the maximum wave amplitude solution approaches the conjugate flow limit (or a front solution), although the so-called wave breaking and shear instability limits are also possible for some parameter ranges.

For two-layer system, Breyiannis *et al.*[12] considered internal waves in a linear shear current numerically using a boundary integral method. Since their focus was on surface waves at the air-water interface, they added wind of constant velocity in the upper layer, resulting in a velocity discontinuity at the interface. Therefore, along with the large density jump that they considered, their results are not directly applicable to internal waves of our interest.

Here, we consider a system of two layers, each of which has constant density and constant vorticity by assuming the detailed vorticity distribution is not important for long internal waves. Solitary wave solutions are computed and compared with those of the irrotational model, and particular attention is paid to wave profiles, wave speeds, and streamlines. This paper is organized as follows. With the governing equations in Sec. II, the strongly nonlinear model is presented in Sec. III and is reduced to a single equation for

[a)]Electronic mail: wychoi@njit.edu

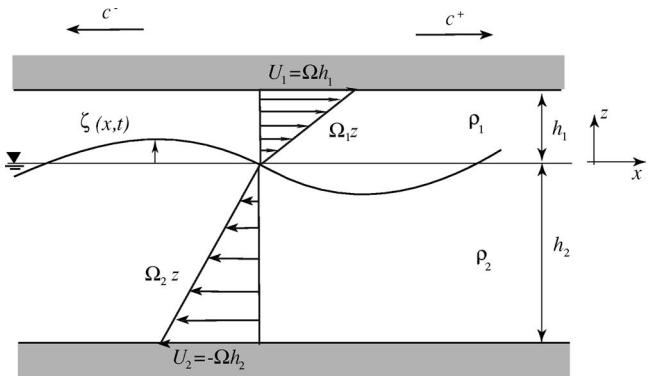

FIG. 1. Internal waves in two-layer system interacting with linear shear currents.

solitary waves. In Sec. IV, using the Boussinesq assumption and assuming vorticity is uniform for simplicity, the properties of large amplitude internal solitary waves propagating in both horizontal directions are described in detail with concluding remarks in Sec. V.

II. GOVERNING EQUATIONS

For an inviscid and incompressible fluid of density ρ_i, the velocity components in Cartesian coordinates (u_i^*, w_i^*) and the pressure p_i^* satisfy the continuity equation and the Euler equations,

$$u_{ix}^* + w_{iz}^* = 0, \tag{2.1}$$

$$u_{it}^* + u_i^* u_{ix}^* + w_i^* u_{iz}^* = -p_{ix}^*/\rho_i, \tag{2.2}$$

$$w_{it}^* + u_i^* w_{ix}^* + w_i^* w_{iz}^* = -p_{iz}^*/\rho_i - g, \tag{2.3}$$

where g is the gravitational acceleration and subscripts with respect to space and time represent partial differentiation. Here, $i=1$ $(i=2)$ stands for the upper (lower) fluid (see Fig. 1) and $\rho_1 < \rho_2$ is assumed for a stable stratification.

The boundary conditions at the interface are the continuity of normal velocity and pressure,

$$\zeta_t + u_1^*\zeta_x = w_1^*, \quad \zeta_t + u_2^*\zeta_x = w_2^*, \quad p_1^* = p_2^* \quad \text{at } z = \zeta(x,t), \tag{2.4}$$

where ζ is the interface displacement. At the upper and lower rigid surfaces, the kinematic boundary conditions are given by

$$w_1^*(x,h_1,t) = 0, \quad w_2^*(x,-h_2,t) = 0, \tag{2.5}$$

where h_1 (h_2) is the undisturbed thickness of the upper (lower) fluid layer.

We assume that the total velocity can be decomposed into a background uniform shear of constant vorticity Ω_i and a perturbation so that

$$u_i^*(x,y,z) = \Omega_i z + u_i(x,z,t), \quad w_i^* = w_i(x,z,t), \tag{2.6}$$

where u_i^* and w_i^* are the total horizontal and vertical velocities, respectively, while u_i and w_i represent the perturbation velocities. From conservation of vorticity, any two-dimensional perturbation to uniform shear flows must be irrotational and, therefore, the perturbation velocities can be written as $u_i = \phi_x$ and $w_i = \phi_z$, where the velocity potential ϕ_i satisfies the Laplace equation $\nabla^2\phi_i = 0$. By substituting into the linearized system of (2.2) and (2.4),

$$\begin{aligned} \phi_1 &= A_1 \cosh[k(z-h_1)]e^{i(kx-\omega t)}, \\ \phi_2 &= A_2 \cosh[k(z+h_2)]e^{i(kx-\omega t)}, \end{aligned} \tag{2.7}$$

the linear dispersion relation between wave speed c and wave number k can be obtained from

$$\begin{aligned} c^2(\rho_1 \coth kh_1 + \rho_2 \coth kh_2) - c(\rho_1\Omega_1 - \rho_2\Omega_2)/k \\ - g(\rho_2 - \rho_1)/k = 0. \end{aligned} \tag{2.8}$$

For long waves $(kh_i \to 0)$, the linear long wave speed is found to be

$$\begin{aligned} c = \frac{h_1h_2(\rho_1\Omega_1 - \rho_2\Omega_2)}{2(\rho_1h_2 + \rho_2h_1)} \\ \pm \sqrt{\frac{h_1^2h_2^2(\rho_1\Omega_1 - \rho_2\Omega_2)^2}{4(\rho_1h_2 + \rho_2h_1)^2} + \frac{gh_1h_2(\rho_2 - \rho_1)}{\rho_1h_2 + \rho_2h_1}}, \end{aligned} \tag{2.9}$$

which, for $\Omega_i = 0$, can be reduced to

$$c = \pm \sqrt{\frac{gh_1h_2(\rho_2 - \rho_1)}{\rho_1h_2 + \rho_2h_1}}. \tag{2.10}$$

III. A STRONGLY NONLINEAR MODEL

For long surface gravity waves in a single layer with constant vorticity, a system of nonlinear evolution equations was derived by Choi[13] by adopting the similar asymptotic expansion method used in Choi and Camassa.[8] Since the detailed derivation of the model can be found in Choi,[13] it will be omitted here.

Assuming the ratio of water depth to the characteristic wavelength is small for long waves, the pressure in (2.3) is expanded to the second order in this small parameter to include the nonhydrostatic pressure effect, which, when combined with (2.1) and (2.2), results in the nonlinear evolution equations for the lower layer,

$$\eta_{2t} - \Omega_2h_2\eta_{2x} + \Omega_2\eta_2\eta_{2x} + (\eta_2\bar{u}_2)_x = 0, \quad \eta_2 = h_2 + \zeta, \tag{3.1}$$

$$\bar{u}_{2t} - \Omega_2h_2\bar{u}_{2x} + \bar{u}_2\bar{u}_{2x} + g\zeta_x = -P_x/\rho_2 + \frac{1}{\eta_2}\left(\frac{2}{3}\eta_2^3G_2\right)_x, \tag{3.2}$$

where $P = p(x,\zeta,t)$ is the pressure at the interface providing coupling with the upper layer, and the depth-averaged velocity $\bar{u}_2$ and the nonhydrostatic pressure effect G_2 are defined by

$$\bar{u}_2(x,t) = \frac{1}{\eta_2}\int_{-h_2}^{\zeta} u_2(x,z,t)\,dz, \tag{3.3}$$

$$G_2(x,t) = \bar{u}_{2xt} - \Omega_2 h_2 \bar{u}_{2xx} + \Omega_2 \eta_2 \bar{u}_{2xx} + \bar{u}_2 \bar{u}_{2xx} - (\bar{u}_{2x})^2. \tag{3.4}$$

The kinematic equation (3.1) is exact, while the dynamic equation (3.2) contains an error of $O(\epsilon^4)$, where ϵ is defined by the ratio of water depth to the characteristic wavelength. The second term of the right-hand side of (3.2) represents the nonlinear dispersive effect of large amplitude internal waves.

For the upper layer, by simply replacing (ζ, g, Ω) by $(-\zeta, -g, -\Omega)$ and the subscript 2 by 1, we can obtain an appropriate set of equations. Then, the complete set of equations for the four unknowns $(\zeta, \bar{u}_1, \bar{u}_2, P)$ is, in dimensional form, given by

$$\eta_{it} + U_i \eta_{ix} - \frac{U_i}{h_i} \eta_i \eta_{ix} + (\eta_i \bar{u}_i)_x = 0, \tag{3.5}$$

$$\bar{u}_{i_t} + U_i \bar{u}_{ix} + \bar{u}_i \bar{u}_{ix} + g\zeta_x = -\frac{1}{\rho_i} P_x + \frac{1}{\eta_i}\left[\frac{\eta_i^3}{3}\left(\bar{u}_{ixt} + U_i \bar{u}_{ixx} - \frac{U_i}{h_i} \eta_i \bar{u}_{ixx} + \bar{u}_i \bar{u}_{ixx} - \bar{u}_{ix}^2 \right) \right]_x, \tag{3.6}$$

where U_i is the velocity at the rigid boundary given by

$$U_1 = \Omega_1 h_1, \quad U_2 = -\Omega_2 h_2. \tag{3.7}$$

For $\Omega_i = 0$, the system given by (3.5) and (3.6) can be reduced to the system of equations of Choi and Camassa.[8]

When computing traveling wave solutions, it is useful to write the horizontal momentum equation (3.6) in the following conserved form:

$$\left(\bar{u}_i + \frac{1}{6} \eta_i^2 \bar{u}_{ixx} \right)_t + \left(U_i \bar{u}_i + \frac{1}{2} \bar{u}_i^2 + g\zeta \right)_x = -\frac{1}{\rho_i} P_x + \left[\frac{\eta_i^2}{2}\left(\bar{u}_{ixt} + \frac{2}{3} U_i \bar{u}_{ixx} - \frac{2}{3} \frac{U_i}{h_i} \eta_i \bar{u}_{ixx} + \frac{2}{3} \bar{u}_i \bar{u}_{ixx} - \bar{u}_{ix}^2 \right) \right]_x, \tag{3.8}$$

or, after multiplying (3.6) by η_i,

$$\left(\eta_i \bar{u}_i - \frac{1}{2} \frac{U_i}{h_i} \eta_i^2 \right)_t + \left[\eta_i U_i \bar{u}_i + \eta_i \bar{u}_i^2 - \frac{1}{2} \frac{U_i^2}{h_i} \eta_i^2 - \frac{U_i}{h_i} \eta_i^2 \bar{u}_i + \frac{1}{3}\left(\frac{U_i}{h_i} \right)^2 \eta_i^3 \right]_x + g \eta_i \zeta_x = -\frac{\eta_i}{\rho_i} P_x + \left[\frac{\eta_i^3}{3}\left(\bar{u}_{ixt} + U_i \bar{u}_{ixx} - \frac{U_i}{h_i} \eta_i \bar{u}_{ixx} + \bar{u}_i \bar{u}_{ixx} - \bar{u}_{ix}^2 \right) \right]_x. \tag{3.9}$$

From (3.5), (3.8), and (3.9), it is easy to see that the following three conservation laws hold:

$$\frac{d\mathcal{M}}{dt} \equiv \frac{d}{dt} \int \zeta dx = 0, \tag{3.10}$$

$$\frac{d\mathcal{I}}{dt} \equiv \frac{d}{dt} \int \left(\bar{u}_i + \frac{1}{6} \eta_i^2 \bar{u}_{ixx} \right) dx = 0 \quad (i = 1,2), \tag{3.11}$$

$$\frac{d\mathcal{P}}{dt} \equiv \frac{d}{dt} \left[\sum_{i=1}^{2} \rho_i \int \left(\eta_i \bar{u}_i - \frac{1}{2} \frac{U_i}{h_i} \eta_i^2 \right) dx \right] = 0, \tag{3.12}$$

which physically correspond to conservation laws for mass, irrotationality, and horizontal momentum of a perturbation to the background linear shear current.

In order to find solitary wave solutions traveling with constant speed c, we assume that

$$\zeta(x,t) = \zeta(X), \quad \bar{u}_i(x,t) = \bar{u}_i(X), \quad X = x - ct. \tag{3.13}$$

Substituting (3.13) into (3.5) and integrating once with respect to X yields

$$\bar{u}_i = (c - U_i)\left(1 - \frac{h_i}{\eta_i} \right) + \frac{1}{2} \frac{U_i}{h_i} \eta_i \left(1 - \frac{h_i^2}{\eta_i^2} \right), \tag{3.14}$$

where we have used the boundary conditions at infinity: $\eta_i \to h_i$ and $\bar{u}_i \to 0$ as $|X| \to \infty$. After substituting (3.13) into (3.8) and integrating with respect to X once, Eq. (3.8) can be written as

$$\frac{1}{3} \rho_i \eta_i^2 \left[\left(-c + U_i + \bar{u}_i - \frac{U_i}{h_i} \eta_i \right) \bar{u}_{iXX} - \frac{3}{2} \bar{u}_{iX}^2 \right] = \rho_i \left[(-c + U_i)\bar{u}_i + \frac{1}{2} \bar{u}_i^2 + g\zeta \right] + P, \tag{3.15}$$

where we have used $\bar{u}_{iX}, \bar{u}_{iXX} \to 0$ as $X \to -\infty$. When we subtract (3.15) for $i = 1$ and 2 to eliminate P, we have

$$\sum_{i=1}^{2} \frac{1}{3} \rho_i \eta_i^2 \left[\left(-c + U_i + \bar{u}_i - \frac{U_i}{h_i} \eta_i \right) \bar{u}_{iXX} - \bar{u}_{iX}^2 \right] = \sum_{i=1}^{2} (-1)^{i-1} \rho_i \left[(-c + U_i)\bar{u}_i + \frac{1}{2} \bar{u}_i^2 + g\zeta \right]. \tag{3.16}$$

On the other hand, when we add (3.9) for $i = 1, 2$ and integrate once with respect to X, we have

$$\sum_{i=1}^{2} \frac{1}{3} \rho_i \eta_i^2 \left[\left(-c + U_i + \bar{u}_i - \frac{U_i}{h_i} \eta_i \right) \bar{u}_{iXX} - \bar{u}_{iX}^2 \right] = \sum_{i=1}^{2} \rho_i \left[(-c + U_i + \bar{u}_i)\bar{u}_i - \frac{1}{2}(-c + U_i) \frac{U_i^2}{h_i} \eta_i + \frac{1}{3} \frac{U_i^2}{h_i^2} \eta_i^3 - g(-1)^{i-1}(\eta_i^2 - h_i^2) + h_i P \right], \tag{3.17}$$

where we have used $\eta_1 + \eta_2 = h_1 + h_2$ to obtain the last term in the right-hand side. After using (3.15) with $i = 1$ for P and adding (3.16) and (3.17), the final equation for ζ_X can be found, after a lengthy manipulation, as

$$\zeta_X^2 = \frac{3\zeta^2 (A_1 \zeta^3 + A_2 \zeta^2 + A_3 \zeta + A_4)}{B_1 \zeta^5 + B_2 \zeta^4 + B_3 \zeta^3 + B_4 \zeta^2 + B_5 \zeta + B_6}, \tag{3.18}$$

where

$$A_1 = -\frac{\rho_1}{12}\frac{U_1^2}{h_1^2} + \frac{\rho_2}{12}\frac{U_2^2}{h_2^2},$$

$$A_2 = -\frac{\rho_1}{12}\frac{U_1^2}{h_1^2}(h_2 - 4h_1) - \frac{\rho_2}{12}\frac{U_2^2}{h_2^2}(h_1 - 4h_2) + (\rho_2 - \rho_1)g,$$

$$A_3 = \frac{1}{3}\left(\rho_1\frac{U_1^2}{h_1^2} - \rho_2\frac{U_2^2}{h_2^2}\right)h_1h_2 - c(\rho_1U_1 - \rho_2U_2) + c^2(\rho_1 - \rho_2) + (\rho_2 - \rho_1)g(h_2 - h_1),$$

$$A_4 = -c(\rho_1U_1h_2 + \rho_2U_2h_1) + c^2(\rho_1h_2 + \rho_2h_1) - (\rho_2 - \rho_1)gh_1h_2,$$

$$B_1 = \frac{\rho_1}{4}\frac{U_1^2}{h_1^2} - \frac{\rho_2}{4}\frac{U_2^2}{h_2^2},$$

$$B_2 = \frac{\rho_1}{4}\frac{U_1^2}{h_1^2}(h_2 - 4h_1) + \frac{\rho_2}{4}\frac{U_2^2}{h_2^2}(h_1 - 4h_2),$$

$$B_3 = \rho_1\frac{U_1^2}{h_1^2}(h_1^2 - h_1h_2) - \rho_2\frac{U_2^2}{h_2^2}(h_2^2 - h_1h_2) + c(\rho_1U_1 - \rho_2U_2),$$

$$B_4 = \rho_1\frac{U_1^2}{h_1^2}h_1^2h_2 + \rho_2\frac{U_2^2}{h_2^2}h_1h_2^2 + \rho_1cU_1(h_2 - 2h_1) + \rho_2cU_2(h_1 - 2h_2),$$

$$B_5 = -2ch_1h_2(\rho_1U_1 - \rho_2U_2) + c^2(\rho_1h_1^2 - \rho_2h_2^2),$$

$$B_6 = c^2h_1h_2(\rho_1h_1 + \rho_2h_2).$$

When $U_i=0$, (3.18) becomes the equation for irrotational internal waves (Miyata;[14] Choi and Camassa[8]),

$$\zeta_X^2 = \frac{3\zeta^2\{g(\rho_2 - \rho_1)\zeta^2 + (\rho_2 - \rho_1)[g(h_2 - h_1) - c^2]\zeta + c^2(\rho_1h_2 + \rho_2h_1) - (\rho_2 - \rho_1)gh_1h_2\}}{c^2[(\rho_1h_1^2 - \rho_2h_2^2)\zeta + (\rho_1h_1 + \rho_2h_2)h_1h_2]}. \tag{3.19}$$

For the one-layer case ($\rho_1=0$) (3.18) can be reduced to the model for surface waves in a uniform shear flow,[13]

$$\zeta_X^2 = -\frac{\zeta^2[\zeta^2 + (4 + 12gh_2^2/U_2^2)\zeta + (12h_2^2/U_2^2)(c^2 - cU_2 - gh_2)]}{[\zeta^2 + 2h_2\zeta + 2(c/U_2)h_2^2]^2}, \tag{3.20}$$

where, from (3.7), $U_2=-\Omega_2h_2$.

IV. BOUSSINESQ ASSUMPTION WITH UNIFORM VORTICITY

To further simplify Eq. (3.18), we assume a small density change across the interface (true for most oceanic applications) and use the Boussinesq assumption, so that we can replace $\rho_1=\rho_0-\Delta\rho/2$ and $\rho_2=\rho_0+\Delta\rho/2$ by ρ_0 except for terms proportional to the gravitational acceleration g. Also, for simplicity, uniform vorticity is assumed and, thus, $\Omega_1=\Omega_2\equiv\Omega$. Then, the equation for ζ_X given by (3.18) can be simplified to

$$\zeta_X^2 = \frac{3\zeta^2(A_2\zeta^2 + A_3\zeta + A_4)}{B_2\zeta^4 + B_3\zeta^3 + B_4\zeta^2 + B_5\zeta + B_6}, \tag{4.1}$$

where the coefficients are given by

$$A_2 = \rho_0\Omega^2(h_1 + h_2)/4 + \Delta\rho g,$$

$$A_3 = -\rho_0\Omega c(h_1 + h_2) + \Delta\rho g(h_2 - h_1),$$

$$A_4 = \rho_0c^2(h_1 + h_2) - \Delta\rho gh_1h_2,$$

$$B_2 = -3\rho_0\Omega^2(h_1 + h_2)/4,$$

$$B_3 = \rho_0\Omega^2(h_1^2 - h_2^2) + \rho_0\Omega c(h_1 + h_2),$$

$$B_4 = \rho_0\Omega^2h_1h_2(h_1 + h_2) - 2\rho_0\Omega c(h_1^2 - h_2^2),$$

$$B_5 = -2\rho_0\Omega ch_1h_2(h_1 + h_2) + \rho_0c^2(h_1^2 - h_2^2),$$

$$B_6 = \rho_0c^2h_1h_2(h_1 + h_2).$$

From the fact that the numerator has to vanish at the wave crest where $\zeta=a$ with a being the wave amplitude, the wave speed c can be found, in terms of a, as

$$c = \frac{\Omega a}{2} \pm \sqrt{\frac{g(\Delta\rho/\rho_0)(h_1 - a)(h_2 + a)}{h_1 + h_2}}. \tag{4.2}$$

Notice that, compared with the irrotational ($\Omega=0$) case, the nonlinear wave speed is increased by $\Omega a/2$, while the linear wave speed c_0 given, from (4.2) with $a=0$, by

$$c_0 = \pm\sqrt{\frac{g(\Delta\rho/\rho_0)h_1h_2}{h_1 + h_2}}, \tag{4.3}$$

is unaffected by constant vorticity under the Boussinesq assumption.

As in the irrotational case, when $A_2a^2+A_3a+A_4=0$ in the numerator of (4.1) has double roots, we have the maximum wave amplitude, at which, instead of a solitary wave, a front solution appears and beyond which no solitary wave solution exists. This condition can be written as $A_3^2=4A_2A_4$ to yield the following expression for the maximum wave speed c_m:

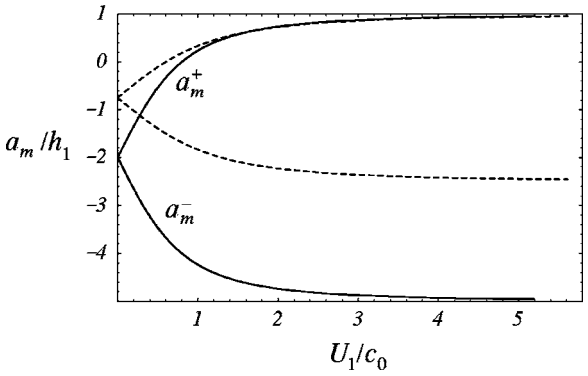

FIG. 2. Maximum wave amplitude a_m given by (4.5) for varying U_1/c_0, where $U_1=\Omega h_1$ and c_0 is the linear long internal wave speed defined by (4.3): - - -, $h_2/h_1=2.5$; —, $h_2/h_1=5$. The density ratio is $\rho_2/\rho_1=1.001$, and the superscripts + and − indicate the waves propagating in the positive and negative x directions, respectively.

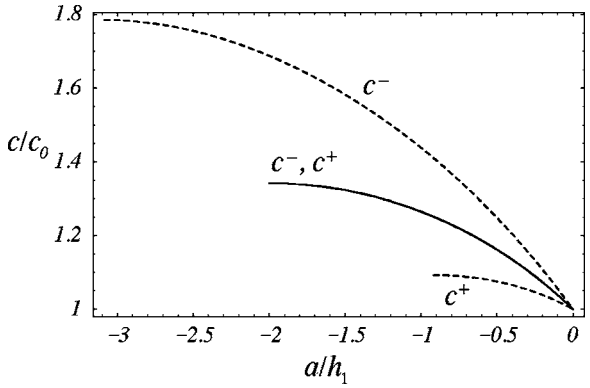

FIG. 3. Wave speed c vs wave amplitude a given by (4.2) for the case of $h_2/h_1=5$ and $\rho_2/\rho_1=1.001$: —, $U_1/c_0=0$; - - -, $U_1/c_0=0.3464$ (or $\Omega/\sqrt{g/h_1}=0.01$), where $U_1=\Omega h_1$ and c_0 is the linear long internal wave speed defined by (4.3). Notice that $|c^+|=|c^-|$ for $\Omega=0$. The density ratio is $\rho_2/\rho_1=1.001$, and the superscripts + and − indicate the waves propagating in the positive and negative x directions, respectively.

$$c_m^{\pm}=\frac{1}{4}\Big[\Omega(h_1-h_2) \pm \sqrt{4g(\Delta\rho/\rho_0)(h_1+h_2)+\Omega^2(h_1+h_2)^2}\Big]. \tag{4.4}$$

Then, the maximum wave amplitude a_m can be found, from (4.2), as

$$a_m^{\pm}=\frac{2g(\Delta\rho/\rho_0)(h_1-h_2)+2\Omega(h_1+h_2)c_m^{\pm}}{4g(\Delta\rho/\rho_0)+\Omega^2(h_1+h_2)}. \tag{4.5}$$

For $\Omega=0$, the maximum wave speed and the maximum wave amplitude can be reduced to

$$c_m^{\pm}=\pm\tfrac{1}{2}\sqrt{g(\Delta\rho/\rho_0)(h_1+h_2)}, \quad a_m^{\pm}=\tfrac{1}{2}(h_1-h_2), \tag{4.6}$$

which are the results of Choi and Camassa[8] under the Boussinesq assumption.

In this paper, without loss of generality, we assume $\Omega>0$ and consider waves traveling in both positive and negative x directions. The density ratio $\rho_2/\rho_1=1.001$ is chosen for the results presented here, and $h_2>h_1$ is assumed so that a solitary wave of depression is expected, unless Ω is large.

As shown in Fig. 2, when propagating in the negative x direction, the maximum wave amplitude (a_m^-) increases considerably as Ω (or, equivalently, U_1) increases, approaching $-h_2$. On the other hand, when propagating in the positive x direction, the maximum wave amplitude (a_m^+) decreases and its polarity changes as Ω increases. Even though the thickness of the lower layer is greater than that of the upper layer, it is possible for a solitary wave of elevation to exist, for example, when $\Omega h_1/c_0>0.8$ for $h_2/h_1=5$. Figure 2 also shows that, for $\Omega\neq 0$, the maximum wave amplitude can be zero, implying that no solitary wave solution exists, even at a depth ratio different from the critical ratio ($h_2/h_1=1$) for $\Omega=0$.

From Fig. 3, for a given depth ratio and $\Omega h_1/c_0$, it can be seen that the wave speed (c^-) is greater for the wave traveling in the negative x direction compared with that of the irrotational solitary wave of same amplitude, while the opposite is true for the wave traveling in the positive x direction.

As shown in Fig. 4(a), solitary wave profiles of $a/h_1=-0.5$ are obtained by solving (4.1) numerically using MATHEMATICA, and it is found that the solitary wave traveling in the positive x direction is wider than that of the solitary wave

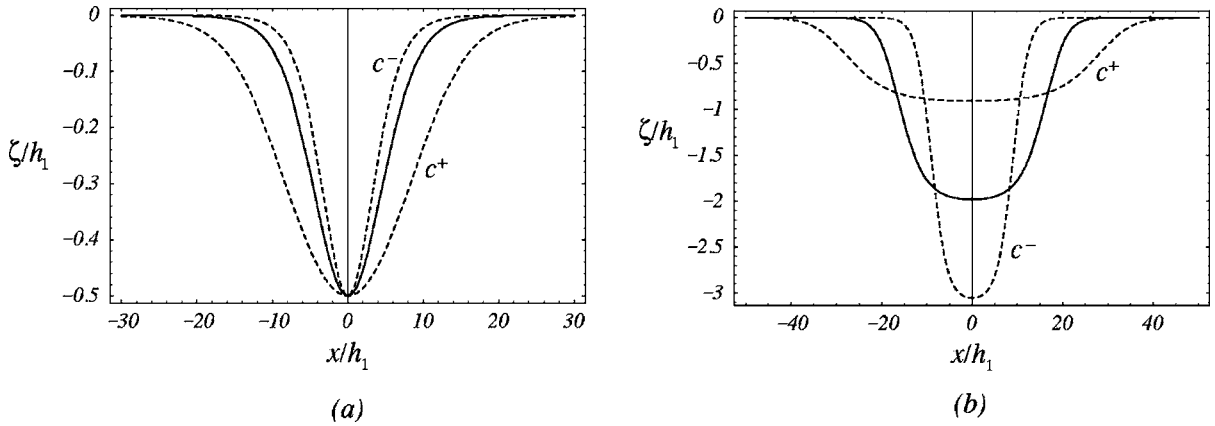

FIG. 4. Solitary wave profiles for $U_1/c_0=0.3464$ ($\Omega/\sqrt{g/h_1}=0.01$, dashed line), where $U_1=\Omega h_1$, compared with those for $\Omega=0$ (solid line) for $\rho_2/\rho_1=1.001$ and $h_2/h_1=5$. (a) $a/h_1=-0.5$, (b) $a=0.99a_m$, where $a_m/h_1\approx-0.9165$ and -3.0835 for waves traveling to the right and left, respectively.

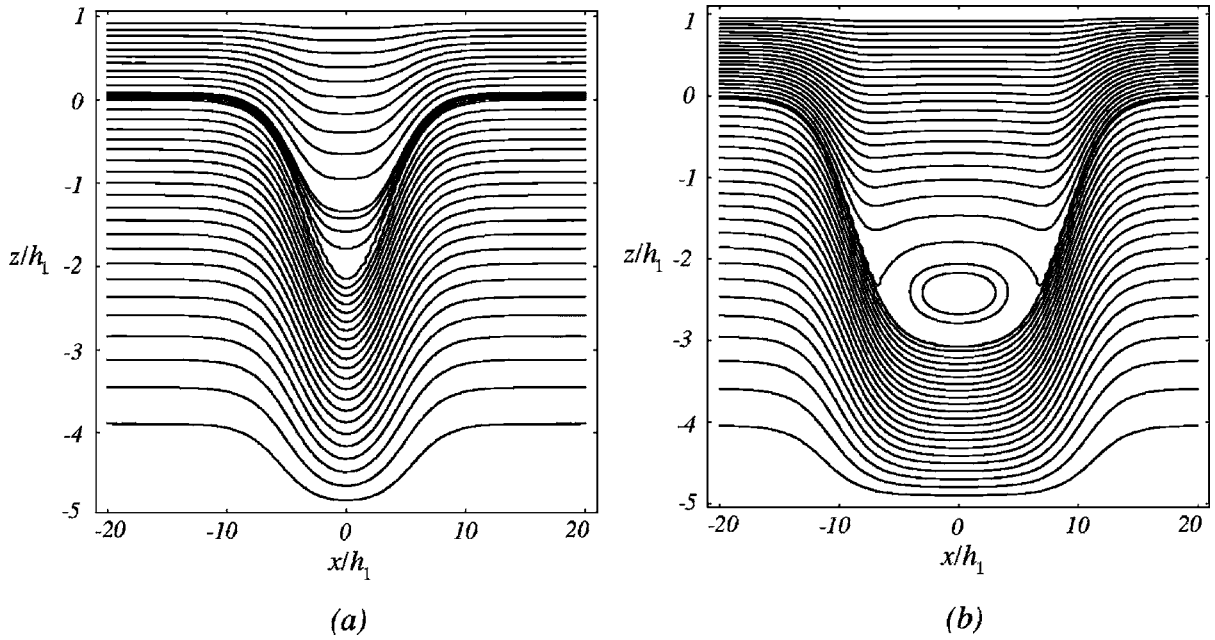

FIG. 5. Streamlines for a solitary wave propagating in the negative x direction, without and with a recirculating eddy, for $U_1/c_0=0.3464$ ($\Omega/\sqrt{g/h_1}=0.01$, dashed line), $\rho_2/\rho_1=1.001$, and $h_2/h_1=5$: (a) $a=0.7a_m$ and (b) $a=0.99a_m$, where $a_m/h_1\approx-3.0835$. Notice that the frame of reference moving with the solitary wave is used and the vertical scale is exaggerated.

traveling in the negative x direction. Also, as can seen in Fig. 4(b), the wave profiles near the maximum wave amplitudes are very different for two waves traveling in opposite directions. For example, the wave propagating in the negative x direction is much taller and narrower, which is consistent with the numerical solution of Stastna and Lamb[11] for continuously stratified shear flows.

It is interesting to notice that, when a large amplitude wave is traveling in the negative x direction, it is possible for a recirculating eddy to appear at the wave crest. Figure 5 shows the streamlines for solitary waves of two different wave amplitudes. A well-defined stationary recirculating eddy can be observed for $a/h_1=0.99a_m$, where $a_m/h_1=-3.0835$, as shown in Fig. 5(b), while it disappears for $a/h_1=0.7a_m$. In the absence of shear, the presence of a stationary recirculating eddy was observed previously in two-layer system with a constant Brunt-Väisälä frequency along with a density jump across the interface by Voronovich.[15]

The criterion of existence of this recirculating eddy can be found from the fact that a stagnation point where the velocity vanishes should appear in the upper layer, more specifically, $a\leqslant z\leqslant 0$. At the leading order, the total stream function Ψ can be approximated by

$$\Psi(X,z)=\begin{cases}\frac{1}{2}\Omega z^2-cz+\bar{u}_1(X)(z-h_1) & \text{for} \quad \zeta(X)\leqslant z\leqslant h_1,\\ \frac{1}{2}\Omega z^2-cz+\bar{u}_2(X)(z+h_2) & \text{for} \quad -h_2\leqslant z\leqslant \zeta(X).\end{cases} \tag{4.7}$$

Then, the total horizontal velocity in the upper layer at the origin ($X=0$) can be found, after substituting (3.14) for $\bar{u}_1$, as

$$\frac{\partial\Psi}{\partial z}=\Omega z-c^-+\bar{u}_1(0)$$
$$=\Omega z-\frac{1}{2}\Omega a+h_1\sqrt{\frac{g(\Delta\rho/\rho_0)(h_2+a)}{(h_1+h_2)(h_1-a)}}, \tag{4.8}$$

from which the vertical location of a stagnation point z_0 can be found as

$$z_0=\frac{a}{2}-\frac{h_1}{\Omega}\sqrt{\frac{g(\Delta\rho/\rho_0)(h_2+a)}{(h_1+h_2)(h_1-a)}}. \tag{4.9}$$

For this stagnation point to lie in $a\leqslant z_0\leqslant 0$, the following inequality between a and Ω must be satisfied:

$$\Omega\geqslant-\frac{2h_1}{a}\sqrt{\frac{g(\Delta\rho/\rho_0)(h_2+a)}{(h_1+h_2)(h_1-a)}}, \tag{4.10}$$

which is shown in Fig. 6.

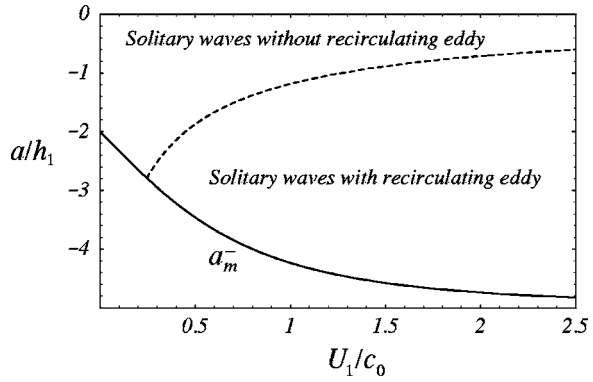

FIG. 6. Domain of existence of recirculating eddy for $\rho_2/\rho_1=1.001$ and $h_2/h_1=5$. Solid line: the maximum wave amplitude given by (4.5); dashed line: Eq. (4.10).

V. CONCLUDING REMARKS

We have studied large amplitude internal solitary wave solutions in a linear shear current using the strongly nonlinear asymptotic model. It is found that, even for small background vorticity, the wave characteristics are significantly different for waves traveling in opposite directions. The background linear shear current changes not only the wave speed, but also the wave shape drastically. Therefore, the knowledge of background currents is essential for the accurate interpretation of an increasing number of field measurements.

Validity of the strongly nonlinear model in the absence of shear has been examined by Ostrovsky and Grue[16] and Camassa *et al.*[9] It was found that solitary wave solutions of the model show excellent agreement with Euler solutions and laboratory/field experiments in shallow configuration in which the depth ratio h_2/h_1 is less than roughly 10. The model proposed here is therefore expected to be valid for the same depth ratio range. As the thickness of one layer is much greater than the other, a deep configuration model similar to that in Choi and Camassa[8] should be adopted, although its validity might be limited to intermediate wave amplitudes for a fixed depth ratio.[9]

Here, a simple, uniform vorticity distribution is adopted and a similar approach used here can be applied to a more general vorticity distribution which might be approximated by the stack of constant vorticity layers.

ACKNOWLEDGMENT

This work was supported in part by the U.S. Office of Naval Research through Grant No. N00014-05-1-0273.

[1] J. F. Lynch and P. Dahl, "Special Issue on science and engineering advances in exploring the Asian marginal seas," IEEE J. Ocean. Eng. **29** (2004).
[2] L. A. Ostrovsky and Y. A. Stepanyants, "Internal solitons in laboratory experiments: Comparison with theoretical models," Chaos **15**, 037111 (2005).
[3] K. R. Helfrich and W. K. Melville, "Long nonlinear internal waves," Annu. Rev. Fluid Mech. **38**, 395 (2006).
[4] K. G. Lamb, "Numerical experiments of internal wave generation by strong tidal flow across a finite amplitude bank edge," J. Geophys. Res. **99**, 843 (1994).
[5] J. Grue, H. A. Friis, E. Palm, and P. O. Rusas, "A method for computing unsteady fully nonlinear interfacial waves," J. Fluid Mech. **351**, 223 (1997).
[6] M. Miyata, "Long internal waves of large amplitude," in *Proceedings of the IUTAM Symposium on Nonlinear Water Waves*, edited by H. Horikawa and H. Maruo (Tokyo, Japan, 1988), p. 399.
[7] W. Choi and R. Camassa, "Long internal waves of finite amplitude," Phys. Rev. Lett. **77**, 1759 (1996).
[8] W. Choi and R. Camassa, "Fully nonlinear internal waves in a two-fluid system," J. Fluid Mech. **396**, 1 (1999).
[9] R. Camassa, W. Choi, H. Michallet, P.-O. Rusås, and J. K. Sveen, "On the realm of validity of strongly nonlinear asymptotic approximations for internal waves," J. Fluid Mech. **549**, 1 (2006).
[10] S. A. Maslowe and L. G. Redekopp, "Long nonlinear waves in stratified shear flows," J. Fluid Mech. **101**, 321 (1980).
[11] M. Stastna and K. G. Lamb, "Large fully nonlinear internal solitary waves: The effect of background current," Phys. Fluids **14**, 2987 (2002).
[12] G. Breyiannis, V. Bontozoglou, D. Valougeorgis, and A. Goulas, "Large-amplitude interfacial waves on a linear shear flow in the presence of a current," J. Fluid Mech. **249**, 499 (1993).
[13] W. Choi, "Strongly nonlinear long gravity waves in uniform shear flows," Phys. Rev. E **68**, 026305 (2003).
[14] M. Miyata, "An internal solitary wave of large amplitude," La Mer **23**, 43 (1985).
[15] A. G. Voronovich, "Strong solitary internal waves in a 2.5-layer model," J. Fluid Mech. **474**, 85 (2003).
[16] L. A. Ostrovsky and J. Grue, "Evolution equations for strongly nonlinear internal waves," Phys. Fluids **15**, 2934 (2003).